

DIRECT NUMERICAL SIMULATION OF SPATIALLY DEVELOPING TURBULENT BOUNDARY LAYER FOR SKIN FRICTION DRAG REDUCTION BY WALL SURFACE-HEATING OR COOLING

Yukinori Kametani

Department of mechanical engineering
Keio University
Hiyoshi 3-14-1, Kohoku-ku, Yokohama 223-8522, Japan.
kametani@fukagata.mech.keio.ac.jp

Koji Fukagata

Department of mechanical engineering
Keio University
Hiyoshi 3-14-1, Kohoku-ku, Yokohama 223-8522, Japan.
fukagata@mech.keio.ac.jp

ABSTRACT

Direct numerical simulation (DNS) of spatially developing turbulent boundary layer with uniform heating or cooling is performed aiming at skin friction drag reduction. The Reynolds number based on the free-stream velocity, the 99% boundary layer thickness at the inlet and the kinematic viscosity is set to be 3000 and the Prandtl number is 0.71. A constant temperature is imposed on the wall. The Richardson number for the buoyancy Ri is varied in the range of $-0.02 \leq Ri \leq 0.02$. The DNS results show that uniform cooling (UC) reduces the skin friction drag, while uniform heating (UH) enhances it. The trend is similar to that in channel flow studied by Iida & Kasagi (1997) and Iida et al. (2002). An analysis using the FIK identity clarifies that UC can reduce skin friction drag by stabilizing the turbulent in the flow, while UH has the opposite trends; UC generates stable density stratification and UH does unstable one.

INTRODUCTION

The large skin friction drag of turbulent flow has a huge impact on the global environment. Its reduction is required, in particular, for reducing fuel consumption in major transportation systems such as aircrafts, trains, and ships. Various approaches for the friction drag reduction have been examined, but a practical method is still being explored. Moreover, despite its practical importance, control of external flows such as a spatially developing boundary layer has not been well studied as compared to that of internal flows.

The buoyancy is considered one of the possible means to generate a body force to reduce the skin friction drag. Iida & Kasagi (2002) and Iida et al. (1997) performed direct numerical simulations of turbulent channel flow under stable and unstable density stratification, respectively. They found that, under the stable density stratification, the turbulence was sup-

pressed and the skin friction drag was decreased because of the generation of internal gravity waves; it is possible to re-laminarize the flow at a large amplitude of Richardson number. Under a weakly unstable density stratification, the skin friction drag was reduced due to diminishing of streamwise vortex near the wall. At larger Richardson numbers, however, large-scale thermal plumes were formed and the activated turbulence increased the skin friction drag.

The local skin friction coefficient in a spatially developing boundary layer, c_f , is mathematically decomposed into the following four terms (Fukagata et al., 2002):

$$\begin{aligned} c_f(x) &= c^\delta(x) + c^T(x) + c^C(x) + c^D(x) \\ &= \frac{4(1 - \delta_m)}{Re_\delta} \\ &\quad + 2 \int_0^1 2(-\overline{u'^*v'^*})(1 - y^*) dy^* \\ &\quad + 2 \int_0^1 2(-U^*V^*)(1 - y^*) dy^* \\ &\quad + 2 \int_0^1 \left(\frac{\partial U^*U^*}{\partial x^*} + \frac{\partial u'^*u'^*}{\partial x^*} \frac{1}{Re_\delta} \frac{\partial^2 U^*}{\partial x^{*2}} \right) dy^*, \end{aligned} \quad (1)$$

where the terms in the right hand side represent the effects of boundary layer thickness, Reynolds stress, mean convection, and spatial development, respectively. This identity equation (referred to as the FIK identity) enables us to make strategies for skin friction drag reduction control from a physical viewpoint.

Kametani & Fukagata (in press) performed direct numerical simulation (DNS) of spatially developing turbulent boundary layer with uniform blowing or suction. They found that uniform blowing from the wall reduces the friction drag because the mean convection term, $c^C(x)$, works as a reduc-

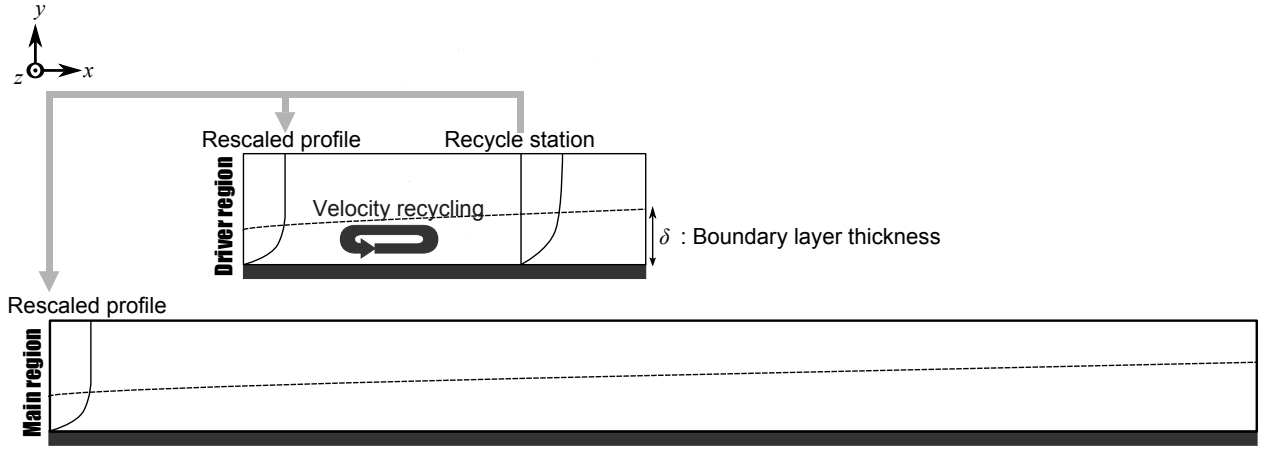


Figure 1. Computational domain

tion factor on drag. Uniform blowing, however, is hardly realized in practice. Body force is considered more practical than the blowing and suction often assumed in the previous studies. For instance, buoyancy can easily be generated by wall surface-heating or cooling. In the present study, DNS of a spatially developing turbulent boundary layer is performed with wall-surface heating and cooling. The effects of heating or cooling on the friction drag is quantitatively discussed by using the FIK identity and their mechanisms are clarified.

DIRECT NUMERICAL SIMULATION

The governing equations are the incompressible continuity, Navier-Stokes and energy equations:

$$\frac{\partial u_i^*}{\partial x_i^*} = 0, \quad (2)$$

$$\frac{\partial u_i^*}{\partial t^*} = -\frac{\partial u_i^* u_j^*}{\partial x_j^*} - \frac{\partial p^*}{\partial x_i^*} + \frac{1}{Re_{\delta_0}} \frac{\partial^2 u_i^*}{\partial x_j^* \partial x_j^*} + Ri\theta^* \delta_{i2}^k, \quad (3)$$

$$\frac{\partial \theta^*}{\partial t^*} = -\frac{\partial u_i^* \theta^*}{\partial x_i^*} + \frac{1}{RePr} \frac{\partial^2 \theta^*}{\partial x_i^* \partial x_i^*}. \quad (4)$$

The buoyancy is taken into account by using the Boussinesq approximation. The superscript * denotes the variables nondimensionalized based on the free-stream velocity, U_∞ , the 99% boundary layer thickness at the inlet, δ_0 , and the temperature difference between free-stream and wall, $\Delta\theta$. The Reynolds number is $Re_{\delta_0} = U_\infty \delta_0 / \nu = 3000$. Furthermore, δ_{i2}^k denotes the Kronecker's delta working on wall normal direction.

The DNS code is based on that of Fukagata et al. (2006) and adapted to boundary layer (Kametani & Fukagata, in press). The computation domain is illustrated in Fig. 1. A driver part is used in order to make the inlet velocity field. The recycle method of Lund et al. (1998) is adopted therein. The streamwise, wall-normal and spanwise lengths of the control part are $(L_x, L_y, L_z) = (3\pi\delta_0, 3\delta_0, \pi\delta_0)$. The corresponding numbers of grid points are $(N_x, N_y, N_z) = (512, 96, 128)$. The convective boundary condition is adopted for the outlet boundary conditions for velocity and temperature. No-slip

and isothermal (i.e., $\theta_{wall} = \theta_{ctr}$) conditions are adopted on the wall. At the upper boundary of the computational domain, the following boundary condition is imposed:

$$\left. \frac{\partial u^*}{\partial y^*} \right|_{up^*} = \left. \frac{\partial v^*}{\partial y^*} \right|_{up^*} = \left. \frac{\partial w^*}{\partial y^*} \right|_{up^*} = 0, w_{up}^* = 0. \quad (5)$$

As for the pressure field, the Neumann and Navier-Stokes Characteristic boundary conditions (Miyachi et al., 1996) are applied at the upper boundary/wall and inlet/outlet, respectively, in order to suppress the unphysical reflection. The control parameter in the present study is the Richardson number, i.e.,

$$Ri = \frac{g\beta\delta_0\Delta\theta}{U_\infty^2}, \quad (6)$$

where g and β denote the gravitational acceleration and the coefficient of volumetric expansion, respectively, and set to be $Ri = 0.01$ & 0.02 in the uniform heating case and $Ri = -0.01$ & -0.02 in the uniform cooling case. Moreover, the wall temperature varies gradually at $0 \leq x/\delta_0 \leq \pi$ by using a hyperbolic function and becomes constant downstream.

RESULT AND DISCUSSION

Visualization

The UC controlled flow field is visualized in Fig. 2 with isosurfaces of the second invariant of velocity gradient tensor, wall shear stress, streamwise velocity and thermal boundary layer thickness. The thermal boundary layer is found to form gradually and become turbulent in the downstream region. Although it is difficult to find the internal gravity wave in the thermal boundary layer because of the low amplitude of 'Ri' (see Fig. 7 of Iida et al. 2002), the vortices are observed to diminish at downstream locations.

STATISTICS

Figure 3 shows the local friction coefficient c_f as a function of streamwise distance from the inlet. It is found that

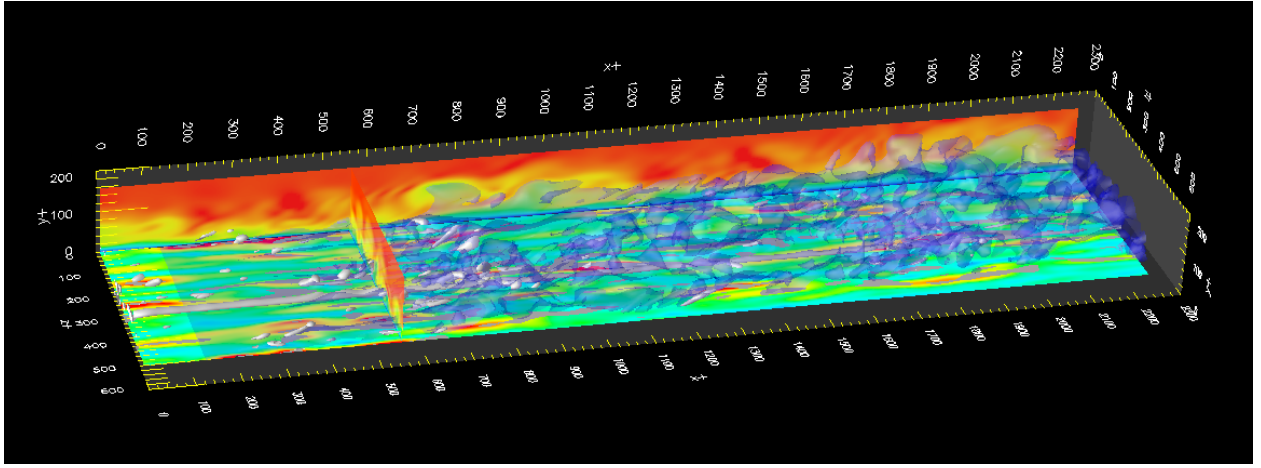


Figure 2. Instantaneous flow field in the uniform cooling case. The contours on the wall and side plane denotes the wall shear stress and the streamwise velocity u , respectively. The blue iso-surface is the 99% thermal boundary layer thickness. The vortex cores are represented in white.

the skin friction drag is reduced by uniform cooling, while enhanced by heating. The amplitude of buoyancy, Ri , affects on the profiles: the larger amplitude results in larger reduction/enhancement of skin friction drag. The trend is basically similar to that in a channel flow studied by Iida & Kasagi (1997) and Iida et al. (2002). In contrast to their studies, however, the present cases of uniform heating, i.e. unstable density stratification, always resulted in increase of skin friction drag. These profiles in Fig. 3 also show that the friction coefficient converges around $x/\delta_0 \geq 4\pi$. At the end of the present computational domain, it is supposed that a numerical oscillation appears in the range of $8\pi \leq x/\delta_0 \leq 9\pi$, especially in UH controlled case.

The mean streamwise velocity profiles at $Re_{\delta_m,nc} = 430$ are shown in Fig. 4, where $Re_{\delta_m,nc}$ denotes the Reynolds number based on U_∞ , ν , and the momentum thickness δ_m and the subscript nc denotes the uncontrolled case. Compared to the uncontrolled case, the profiles are shifted away from the wall by UC and toward to the wall by UH. This is, again, similar to the case of channel flow under constant pressure gradient (Iida & Kasagi, 1997; Iida et al., 2002). Moreover, as illustrated in Fig. 4, the momentum thickness becomes thinner by UC. Namely, the momentum defect is decreased by UC as if the Reynolds number were decreased.

The Reynolds shear stress and viscous shear stress are shown in Fig. 6. It can be seen that the UC control reduces the viscous shear stress, while the UH control enhances it. On the other hand, the Reynolds shear stress is also reduced by cooling, while increased by heating. These results suggest that the vortical motion in the vicinity of wall is suppressed and the flow is stabilized by UC, while the UH destabilizes the turbulence. Namely, UC forms stable density stratification, while UH does unstable one. This trend agrees with the case of zero-net-flux blowing/suction (Fukagata et al., 2002), in which the suppression of turbulence near the wall results in the reduction of skin friction drag.

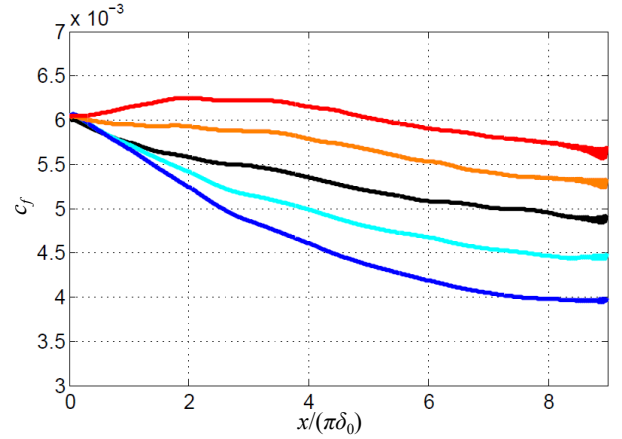


Figure 3. Local friction coefficient, c_f . Black, no control; red, $Ri = 0.02$; orange, $Ri = 0.01$; blue, $Ri = -0.02$; light blue, $Ri = -0.01$.

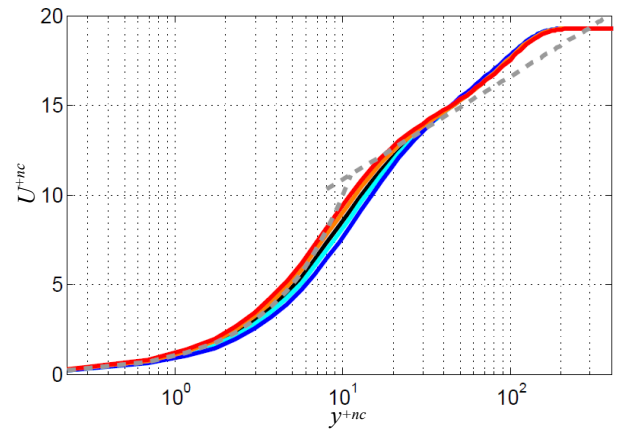


Figure 4. Streamwise mean velocity at $Re_{\delta_m,nc} = 430$ in wall units of uncontrolled case. Black, no control; red, $Ri = 0.02$; orange, $Ri = 0.01$; blue, $Ri = -0.02$; light blue, $Ri = -0.01$.

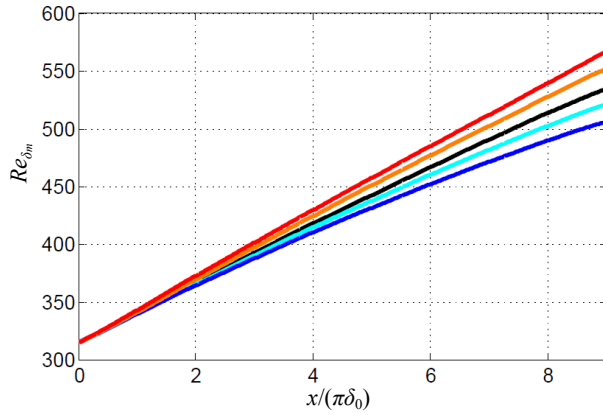


Figure 5. Momentum thickness as Re_{δ_m} . Black, no control; red, $Ri = 0.02$; orange, $Ri = 0.01$; blue, $Ri = -0.02$; light blue, $Ri = -0.01$.

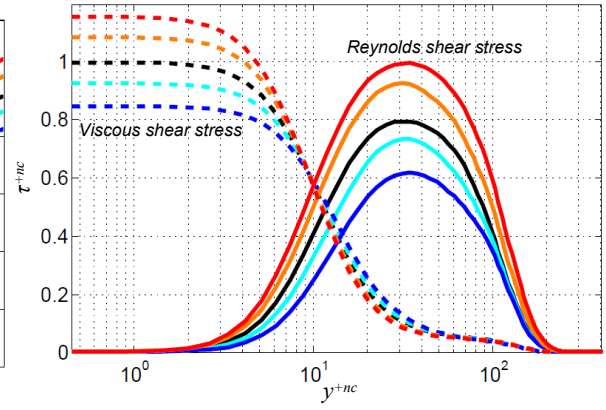


Figure 6. Shear stresses at $Re_{\delta_m,nc} = 430$. Solid line, Reynolds shear stress; dashed line, viscous stress. Black, no control; red, $Ri = 0.02$; orange, $Ri = 0.01$; blue, $Ri = -0.02$; light blue, $Ri = -0.01$.

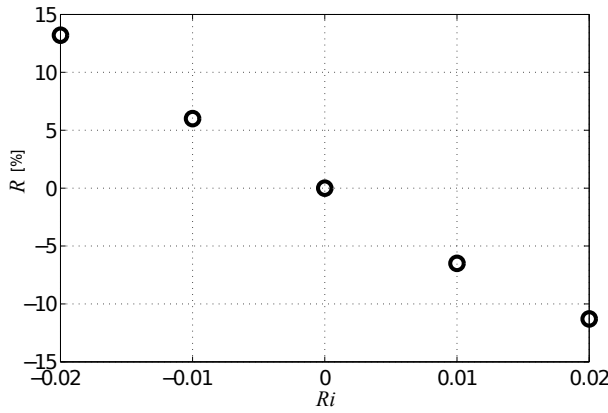


Figure 7. Drag reduction rate as a function of control amplitudes.

GLOBAL SKIN FRICTION DRAG

Figure 7 shows the drag reduction rate R , defined as

$$R = \frac{C_{f,nc} - C_{f,ctr}}{C_{f,nc}}, \quad (7)$$

where $C_{f,nc}$ and $C_{f,ctr}$ denote the global friction coefficients in the uncontrolled case and the controlled case, respectively. In the present study, $R = 13.2\%$ is achieved in the cooling case at $Ri = -0.02$, while $R = -11.3\%$ in the heating case. The figure suggests that there is linear relationship between the control amplitude and the drag reduction rate in the range performed here.

Similarly to the local friction coefficient, the global friction coefficient C_f can be decomposed into four terms by integrating the FIK identity, i.e.,

$$\begin{aligned} C_f &= \frac{1}{L_{ctr}} \left[\int_0^{L_{ctr}} c^\delta(x) dx + \int_0^{L_{ctr}} c^T(x) dx + \int_0^{L_{ctr}} c^C(x) dx \right. \\ &\quad \left. + \int_0^{L_{ctr}} c^D(x) dx \right] \\ &= C^\delta + C^T + C^C + C^D. \end{aligned} \quad (8)$$

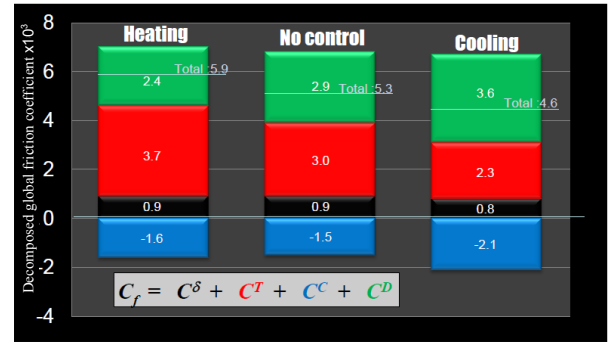


Figure 8. Different dynamical contributions to friction drag ($\times 10^3$).

A comparison of each contribution in uncontrolled, uniform cooling/heating cases at $Ri = 0.02$ & -0.02 are shown in Fig. 8. It clearly shows that the uniform cooling reduces the friction drag by reducing the Reynolds stress term C^T and enhancing the mean convection term C^C . It is also clear that C^C has a negative contribution, viz., it works as a drag reduction factor. The summation of the mean convection term C^C and the spatial development term C^D (which is originally defined as the *spatially development term* in Fukagata et al. (2002)), are almost equal in both controlled cases. It indicates that the effect of drag reduction/enhancement by the control mostly comes from the Reynolds stress term, C^T , similarly to the channel flow (Iida et al. 2002). These are clearly different from the cases with uniform blowing or suction (Kametani & Fukagata, in press), where the friction drag is reduced by uniform blowing and its mechanism is attributed to the negative contribution of mean convection term, C^C .

CONCLUDING REMARKS

Direct numerical simulation of spatially developing turbulent boundary layer with uniform cooling/heating is performed aiming at skin friction drag reduction. The uniform

cooling control achieved 13% of friction drag reduction, while heating resulted in 11% of drag increment. From the shear stress profiles, it is found that uniform cooling reduces both of viscous shear stress and Reynolds shear stress, while uniform heating has opposite trend. Using the FIK identity, the Reynolds stress term is found to be decreased by cooling. Cooling stabilizes the turbulent boundary layer, while heating destabilizes it. These trends also appear in channel flows (Iida & Kasagi 1997, Iida et al. 2002). In both internal and external flows the skin friction drag is reduced by the same mechanism under stable density stratification, This drag reduction mechanism is different from the cases of uniform blowing (Kametani & Fukagata, to appear), where the friction drag was reduced by uniform blowing and it is due to the non-zero flux from the wall.

References

Fukagata, K., Iwamoto, K., & Kasagi, N., 2002, "Contribution of Reynolds stress distribution to the skin friction in wall-bounded flows," *Phys. Fluids*, Vol. 14, pp. L73-L76.

Fukagata, K., Kasagi, N., & Koumoutsakos, P., 2006 "A theoretical prediction of friction drag reduction in turbulent flow by superhydrophobic surfaces," *Phys. Fluids*, Vol. 18, 051703.

Iida, O., Kasagi, N., 1997 "Direct numerical simulation of unstratified turbulent channel flow," *J. Heat Trans-T. ASME.*, Vol. 119-1, pp. 53-61.

Iida, O., Kasagi, N., & Nagano, Y., 2002, "Direct numerical simulation of turbulent channel flow under stable density stratification," *Int. J. Heat Mass Tran.*, Vol. 45-8, pp. 1693-1703.

Kametani, Y. & Fukagata, F., in press, "Direct numerical simulation of spatially developing turbulent boundary layer with uniform blowing or suction," *J. Fluid Mech.*

Lund, T.S., Wu, X., & Squires, K.D., 1998, "Generation of turbulent inflow data for spatially developing boundary layer simulations," *J. Comput. Phys.*, Vol. 140, pp. 233-258.

Miyauchi, T., Tanahashi, M. & Suzuki, M., 1996, "Inflow and outflow boundary conditions for direct numerical simulations," *JSME Int. J. Ser. B*, Vol. 39-2, pp. 305-314.